Int. J. Electrochem. Sci., 7 **(2012)** 11246 - 11256

International Journal of
ELECTROCHEMICAL
SCIENCE
www.electrochemsci.org

Electrochemical Characterization and Metallization of Two Novel Asymmetric Meso-Subtstituted Porphyrins

J.R. Irigoyen[1], *L.M. Blanco*[1,*], *S. T. López*[2]

[1] Universidad Autónoma de Nuevo León, Facultad de Ciencias Químicas, Laboratorio de Electroquímica, Guerrero y Progreso s/n, Col. Treviño, Monterrey 64570, N. L., México.
[2] Universidad Autónoma de Nuevo León, Facultad de Ciencias Químicas, Laboratorio de Electroquímica, Guerrero y Progreso s/n, Col. Treviño, Monterrey 64570, N. L., México.
[*]E-mail: leonyjerez@gmail.com

Received: 23 August 2012 / *Accepted:* 3 October 2012 / *Published:* 1 November 2012

Electrochemical characterization and metallization of two novel meso-susbstituted porphyrins were carried out by sweep and step potential techniques. Redox potentials of 5,10,15-tris(p-chlorophenyl)-20-(2-hydroxy-3-methoxyphenyl)porphyrin and 5,10,15-tris(p-methoxyphenyl)-20-(p-chlorophenyl) porphyrin were identified, and their respective diffusion coefficients at 25 ± 1 °C in CH_2Cl_2 using tetrabutylammonium hexafluorophosphate as supporting electrolyte were determined. The dianion radical formation potentials were found to be influenced by the electrodonor effects of the porphyrin substituents. The metallization process of the porphyrins were carried out by controlled potential electrolysis using an aluminum sacrificial anode to form the metallic ions in situ. The aluminum metalloporphyrin formation of each porphyrin was confirmed by UV-Vis, IR and atomic absorption spectroscopy.

Keywords: Aluminum metalloporphyrin; Electrochemical characterization; Diffusion coefficient; Sacrificial anode; Electrochemical metallization.

1. INTRODUCTION

Porphyrins and porphyrin like compunds are of special interest because of their many technological applications. Porphyrins are capable to be functionalizated and to form metallic complexes. For this reason, they have been studied and used in different areas. They can be used as precursors for new polymers with optical and semiconductor properties or in cancer photodynamic therapy as photosensitizers. This last medical application has conferred special importance to porphyrins [1-3]. The chemical and spectroscopic properties of porphyrins and porphyrin like

compounds can be changed by functionalization of their substituents or by the insertion of a metallic ion in the porphyrin cavity [4,5].

Usually, the traditional synthesis of metalloporphyrins involves long reaction times, high temperatures and reflux conditions, and also the use of a metallic salt that provides the metallic ion of interest. A huge quantity of metalloporphyrins and porphyrin like compounds have been synthesized using this method [6-9]. Nevertheless, different ways of synthesis have been studied; one of them is the electrosynthesis [10,11]. Electrochemical metallization can be carried out by using a sacrificial anode that provides the metallic ion; the free-base and the metallic ions are generated in situ and then they chemically react to form the corresponding metalloporphyrin complexation reaction [11]. Using this electrochemical method, high temperatures and long reaction times can be avoided.

Electrochemical methods have not been widely used to synthesize porphyrins [10, 12-15]. In particular, only a few papers on using a sacrificial anode to form a metalloporphyrin have been published [16,17] in spite of the mild conditions this method requires.

In this paper we report on the electrochemical characterization of two novel asymmetric meso-susbstituted tetraphenyl porphyrins: 5,10,15-tris(p-chlorophenyl)-20-(2-hydroxy-3-methoxyphenyl)porphyrin (A) (Figure 1 (a)), and 5,10,15-tris(p-methoxyphenyl)-20-(p-chlorophenyl)porphyrin (B) (Figure 1 (b)). We also report on the metallization of these porphyrins using an aluminum sacrificial anode under mild conditions, which was performed based on the results of the previous electrochemical characterization.

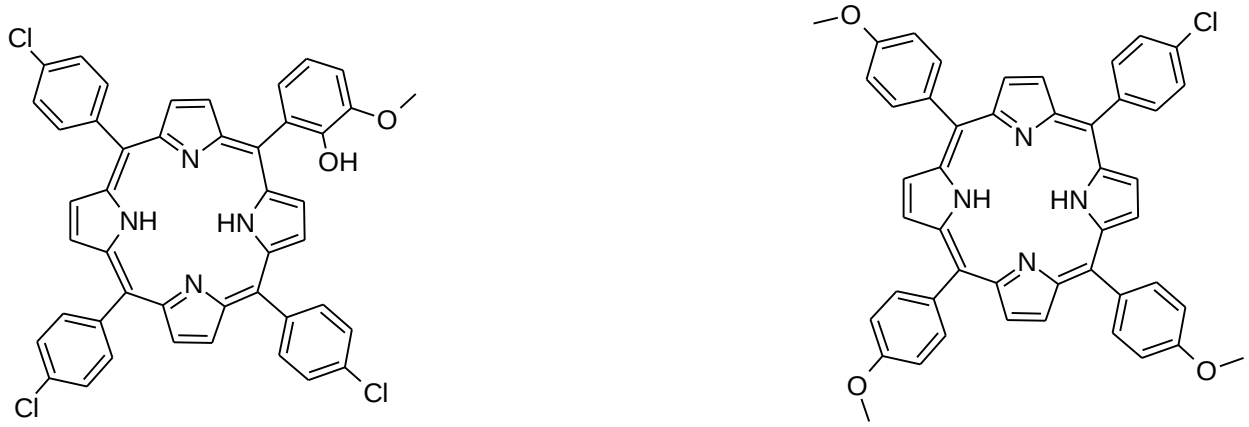

(a) (b)

Figure 1. (a) 5,10,15-tris(p-chlorophenyl)-20-(2-hydroxy-3-methoxyphenyl)porphyrin (A). (b) 5,10,15-tris(p-methoxyphenyl)-20-(p-chlorophenyl)porphyrin (B).

2. EXPERIMENTAL

2.1 Reagents

Porphyrins A and B were synthesized in the Laboratory of Industrial Chemistry, Chemical Sciences School, Autonomous University of Nuevo León, and were used as received. HPLC-grade

dichloromethane from Tedia was used. It was distilled using P_4O_{10} 0.005 g/mL as a solvent and stored over molecular sieves that were previously activated at 134 °C. Hexane from Tedia was used as received. Acetonitrile from Aldrich was used as received. Tetrabuthylammonium hexafluorophosphate (TBAHFP) from Aldrich (≥99.0% purity; electrochemical grade) was used as supporting electrolyte in all experiments. It was dryed at 134 °C for 24 h before preparing all solutions. The precursors of the porphyrins from Aldrich were used for the electrochemical characterization (o-vanillin, p-chlorobenzadehyde and p-methoxybenzaldehyde) as received. All solutions were purged with nitrogen for 15 min before every experiment. Silica gel from J. T. Baker was used as received.

2.2 Equipment

All the electrochemical measurements were carried out in an AUTOLAB potentiostat/galvanostat, PGSTAT 30 model. The bulk electrolyses were carried out in a BAS Epsilon potentiostat/galvanostat. All voltammetric and chronoamperometric measurements were carried out under nitrogen atmosphere using the typical three-electrode configuration. For measurements in organic media, a glassy carbon electrode and two platinum wires were used as working, counter and pseudo-reference electrodes, respectively. The pseudo-reference electrode was externally calibrated with a 5.0 mM Fc/Fc^+ and a 0.1M TBAHFP solution in dichloromethane. For measurements in aqueous media, a glassy carbon electrode, a platinum wire and an Ag/AgCl electrode were used as working, counter and reference electrodes, respectively. For the electrosyntheses, a reticulated vitreous carbon electrode (RVC) was used as working electrode and an electrochemical grade aluminium foil was used as sacrificial anode. Electrosyntheses were performed in an undivided cell. For the determination of the diffusion coefficient, the working electrode was mechanically polished with 0.5 μm alumina, then immersed in distilled water with sonication for 4 min, and finally activated at 1.23 V vs. Ag/AgCl for 5 min in a 1M NaOH solution. This electrode was stored under N_2 between diffusion coefficient experiments. The spectroscopic UV-Vis determinations were carried out in a VARIAN Cary spectrophotometer, model 100Conc Infrared spectra were obtained from a Bruker FT-IR spectrophotometer, model Tensor 27. Atomic absorption determinations were carried out in a GBC spectrophotometer, model 932AA.

2.3 Methods

For the electrochemical characterization, cyclic voltammetry, differential pulse voltammetry and chronoamperometry were performed. For the metallization of each porphyrin, a controlled potential electrolysis was carried out at a potential a few mV higher potential than that identified as the formation potential of the dianion radical. The chromatography in column was carried out using dichlorometane-hexane 7:3 as eluent system.

3. RESULTS AND DISCUSSION

3.1 Electrochemical characterization

In order to identify and correlate each redox process with each part of the molecule, cyclic voltammetries of each porphyrin precursor were performed in CH_2Cl_2. Figure 2 shows the cyclic voltammetries of o-vanillin and p-chlorobenzaldehyde, which were used as precursors for A.

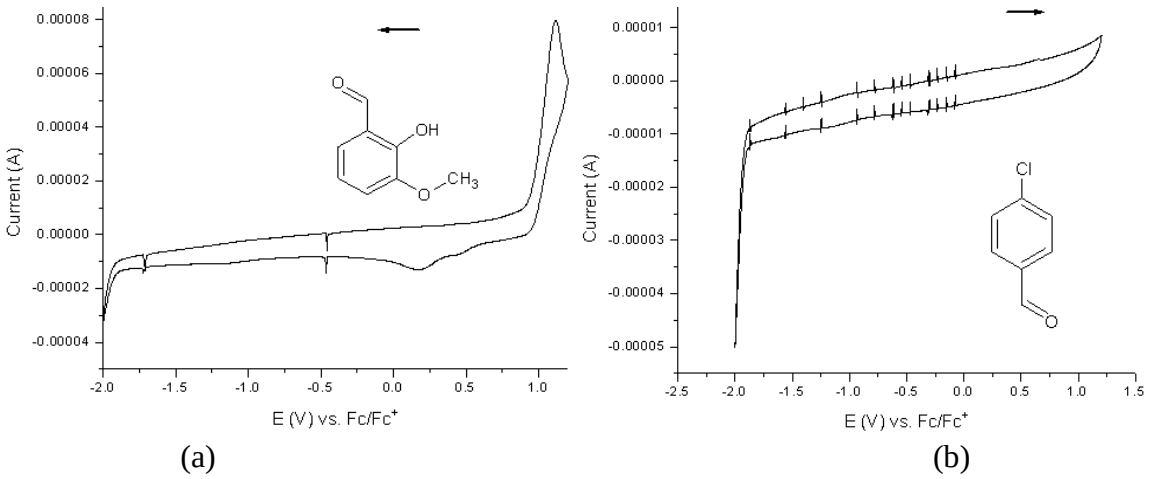

Figure 2. (a) Cyclic voltammetry of o-vanillin 1.97 mM and 0.1M TBAHFP in CH_2Cl_2 at a 100 mV/s scan rate. (b) Cyclic voltammetry of p-chlorobenzaldehyde 2.0 mM and 0.1M TBAHFP in CH_2Cl_2 at a 100 mV/s scan rate.

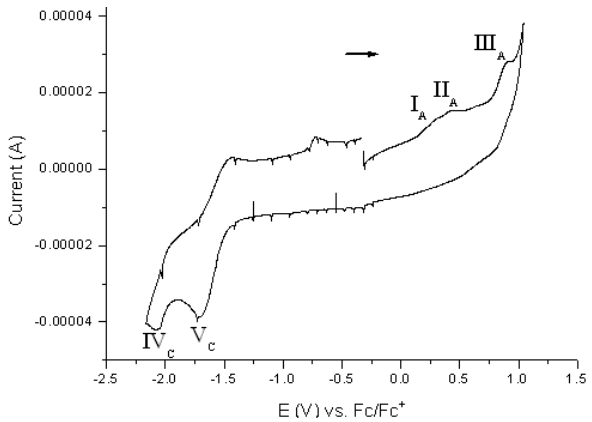

Figure 3. Cyclic voltammetry of A 0.2 mM and 0.1M TBAHFP in CH_2Cl_2 at a 100 mV/s scan rate.

In Figure 2(a), the oxidation process at 0.947 V corresponds to the transformation of the phenolic part in a quinone. The reduction process can be attributed to the reduction of the quinone to a

phenol. From Figure 1(b) we conclude that this aldehyde is not an electroactive agent in these conditions.

Figure 3 shows the redox processes of A. Because under these conditions cyclic voltammetry cannot provide a clear identification of these processes, particularly the oxidation processes of A, differential pulse voltammetry was used [18]. Process III_A is attributed to the two-electron oxidation of the phenolic part [19, 20] in the o-vanillin substituent of A, which corresponds with the processes shown in Figure 2(a). Processes I_A and II_A are associated to the formation of the porphyrin dication radical via two-electron steps, as is reported in several works [21-23]. Processes IV_C and V_C are attributed to a two-electron step formation of the dianion radical [21-23], because the reduction processes are independent of the oxidation processes [17].

The linear behavior for the Randles-Sevcik relationship for A shown in Figure 4(a) indicates that the redox processes are controlled by diffusion. The cyclic voltammetries shown in Figure 4(b) indicate that Process III_A is less favored at high scan rates.

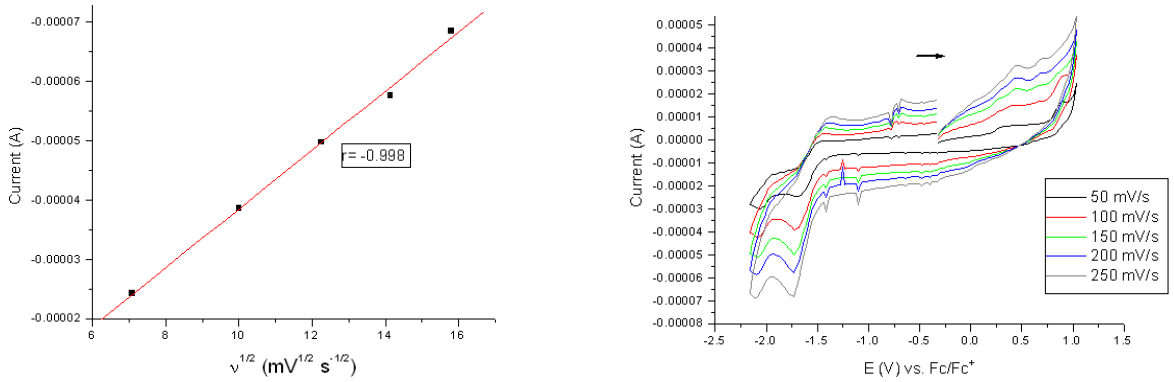

(a) (b)

Figure 4. (a) Randles-Sevcik relationship for A. (b) Cyclic voltammetry of A at five different scan rates.

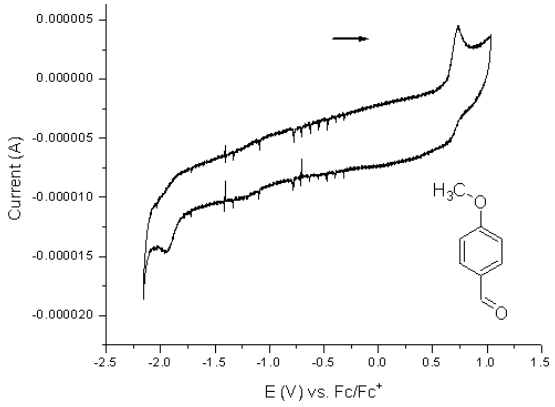

Figure 5. Cyclic voltammetry of p-methoxybenzaldehyde 24.5 mM and 0.1M TBAHFP in CH_2Cl_2 at a 100 mV/s scan rate.

Figure 5 shows the cyclic voltammetry of the p-methoxybenzaldehyde precursor for B.

The oxidation process at 0.727 V shown in Figure 5 can be attributed to the oxidation of the methoxy group present in the molecule and the possible formation of a cation radical, which, in a media lacking nucleophilic species, can be reduced at 0.720 V. The reduction process at -1.941 V can be attributed to the reduction of the aldehyde group to an alcohol.

Figure 6 shows the electrochemical characterization of B, including cyclic and differential pulse voltammetries and the Randles-Sevcik relationship.

Differential pulse voltammetry showed that in II_A there are two processes partially overlapped. Process I_A and the first process of II_A correspond to the formation of the dication radical of the porphyrin, and the second process of II_A corresponds to the oxidation of the methoxy group as described previously. Processes III_C and IV_C correspond to the formation of the dianion radical. These last two processes are independent of the oxidation processes shown in Figure 6(a). B also showed diffusion controlled processes, as shown in Figure 6(c).

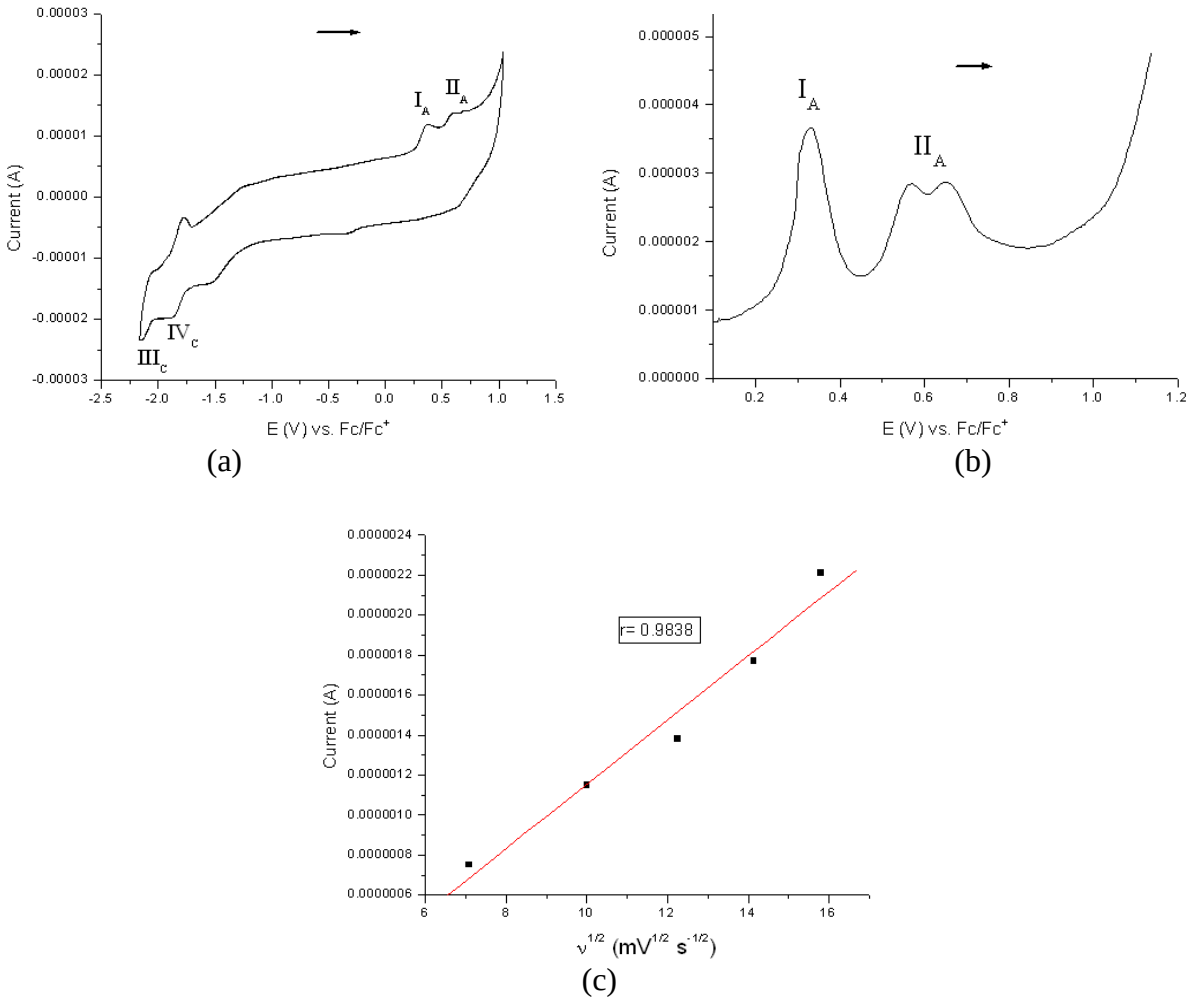

Figure 6. (a) Cyclic voltammetry of B 0.2 mM and 0.1 M in TBAHFP at a 250 mV/s scan rate. (b) Differential pulse voltammetry in the oxidation direction. (c) Randles-Sevcik relationship.

Diffusion coefficients of both porphyrins were determined with a modified version of the procedure described in [24]. We used the Cottrell equation to find the real electrode area and the diffusion coefficients. Because of the volatility of the used organic media, only 10 chronoamperometries were performed. The diffusion coefficient of the reference substance (potassium ferrocyanide) is 0.62 x 10^{-5} cm^2 s^{-1} at 25 °C. The electrode area for the determination of the diffusion coefficient of A was 56.184 ± 0.07 cm^2 and the calculated diffusion coefficient was 0.873 x 10^{-6} ± 0.26 x 10-7 cm^2 s^{-1} at 25 ± 1 °C. The electrode area for the determination of the diffusion coefficient of B was 56.897 ± 0.11 cm^2 and the diffusion coefficient was 0.974 x 10^{-6} ± 0.13 x 10^{-6} cm^2 s^{-1} at 25 ± 1 °C.

The potentials of the redox processes of a porphyrin are affected by its substituents. Figures 7 and 8 show the effect of the substituent on the formation potential of the dianion radical in a porphyrin. For this study, two other porphyrins were considered: 5,10,15,20-tetrakis(p-chlorophenyl)porphyrin (C) and 5,10-bis(p-methoyphenyl)-15,20-bis(p-chlorophenyl) porphyrin (D). Figure 7 shows the formation potential of the dianion radical of porphyrins A, B, C and D (represented by dots) and the voltammograms of these porphyrins. The figure also shows the line representing the linear correlation for the four potentials. The correlation is not good, because the structure of porphyrin C is significantly different from those of A, B, and D. Porphyrin C does not behave as A, B, and D because of its symmetry and the predominant electroatractor effect of its substituents.

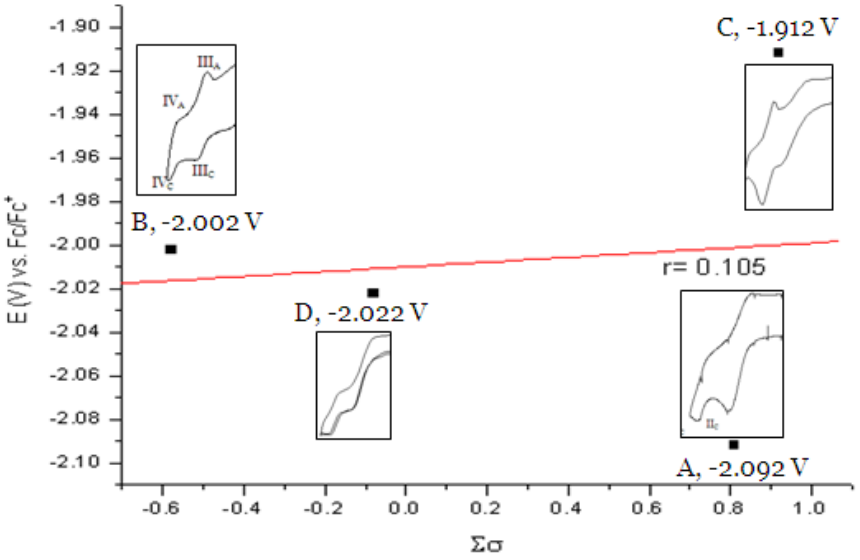

Figure 7. Dianion radical formation potential as a function of the sum of the Hammett sigma constants.

Figure 8 shows the effect of of not considering porphyrin C in the analysis. The linear correlation improves to -0.988. The negative slope in this plot indicates an electrodonor effect in the redox processes of the molecule. The slope is small (-0.064), but this voltage variation is still significant.

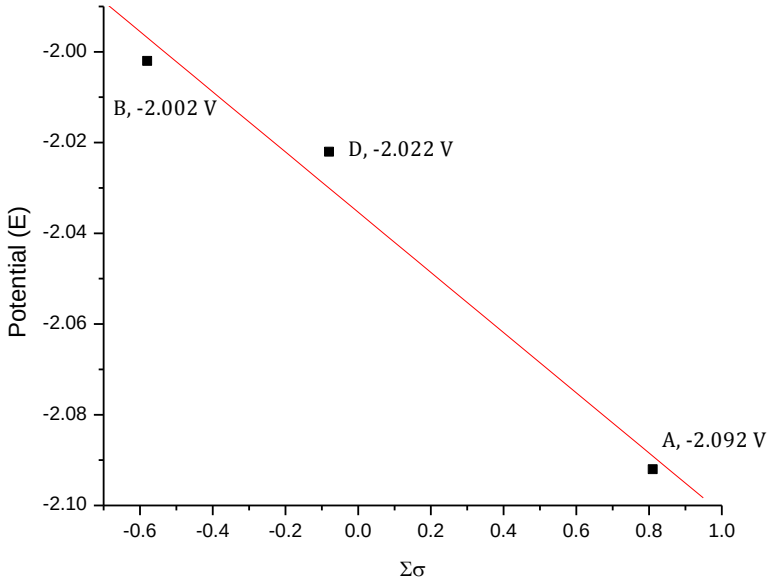

Figure 8. Dianion radical formation potential as a function of the sum of the Hammett sigma constants for porphyrins A, B and D.

Table 1 summarizes the collected data from the electrochemical characterization of porphyrins A and B.

Table 1. Peak potentials for each porphyrin obtained by differential pulse voltammetry. The diffusion coefficients were determined at 25 ± 1 °C.

	Epc1, V	Epc2, V	Epa1, V	Epa2, V	Epa3, V	D x 106 , cm^2 s^{-1}
B	-2.10	-1.79	0.32	0.56	0.65	0.978 ± 0.11
A	-1.99	-1.69	0.45	0.69	0.92	0.873 ± 0.22

3.2 Electrochemical metallization of porphyrins

The controlled potential electrolysis of A using an aluminum foil as sacrificial anode was performed at -2172 mV. The electrochemical efficiency of the process was 94.42%. During the experiment, the characteristic violet color of the free-base porphyrin changed to dark green. The reaction was monitored by TLC and metallization was reached after 45 min. Figure 9 shows the UV-Vis spectra of the free-base porphyrin and the reaction mixture. Figure 9(b) is a mixture of a free-base porphyrin and a metallized porphyrin. A red shift about 24 nm in the Soret band and the pronounced β band can be observed.

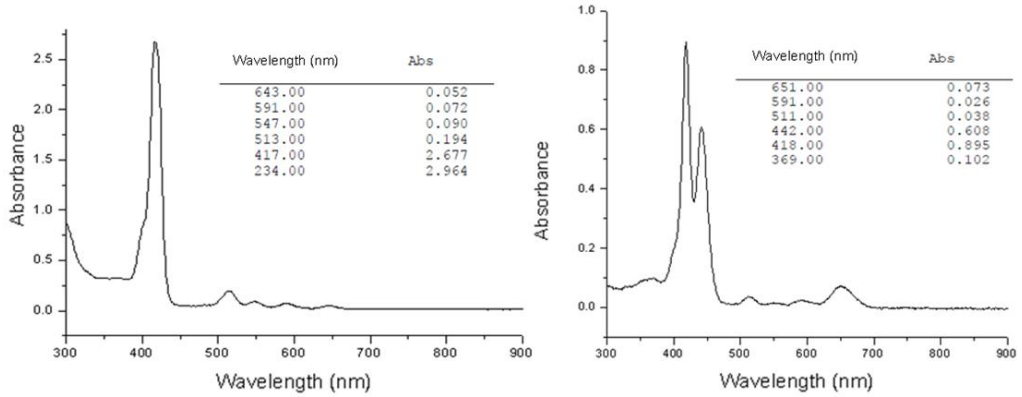

Figure 9. (a) UV-Vis spectrum of the free-base porphyrin. (b) UV-Vis spectrum of the reaction mixture.

Due to the solubility of the product in the reaction media and in other solvents, purification by chromatography in column was the only viable purification procedure for the reaction mixture. However, the obtained product decomposed during the purification. The color of the solution changed to violet and the spectra of its collected fractions were the same as that in Figure 9(a).

The controlled potential electrolysis of B using an aluminum foil as sacrificial anode was performed at -0.215 V. The electrochemical efficiency of the process was 90%. During the experiment, the characteristic violet color of the free-base porphyrin changed to a bright green one. The reaction was monitored by TLC and the metallization was reached after 25 min. However, if the electrolysis continues for more than 30 min, the formed product is destroyed and the free-base porphyrin is obtained again. This behavior is different form that of porphyrin A. Figure 10 shows the UV-Vis spectra of the free-base porphyrin and the reaction mixture. Observe that in Figure 10(b) shows a mixture of free-base porphyrin and metallized porphyrin. Note the red shift of approximately 26 nm in the Soret band and the pronounced β band.

The reaction mixture was evaporated and redissolved in acetonitrile. A bright green solid precipitated and was filtered in vacuum and washed with cold acetonitrile. The yield of the reaction was of 37%. Atomic absorption analysis reveals that the green solid contains 2.49% of aluminum. IR spectrum confirms the absence of the band that corresponds to a N-H tension band due to the protonated pirrols of the free-base porphyrin. The UV-Vis spectrum of the solid is shown in Figure 10(c). The red shift of approximately 32 nm in the Soret band is an expected behavior of a metalloporphyrin [25, 26]. These results, indicated that the bright green solid is the aluminum metalloporphyrin of B.

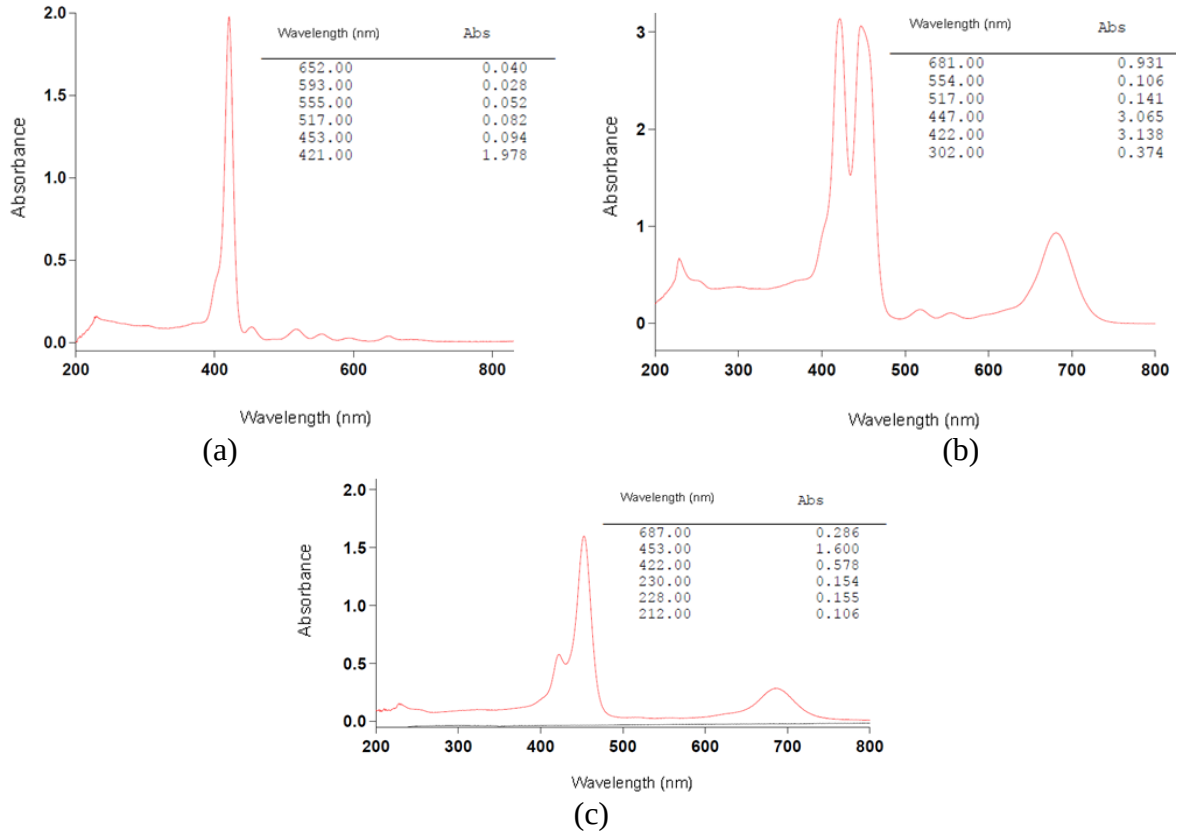

Figure 10. UV-Vis spectra of: (a) Free-base porphyrin. (b) Reaction mixture. (c) Metalloporphyrin.

4. CONCLUSIONS

The electrochemical characterization of both studied porphyrins allowed to determine the formation potentials of the dianion radicals. The electrochemical characterization uncovered other redox processes, which were identified and assigned to each part of the molecule. The diffusion coefficients of porphyrins A and B were determined at 25 ± 1 °C for concentrations of 0.2 mM of both porphyrins and 0.1 M of TBAHFP. Under these conditions, the diffusion coefficient of B is greater than that of A. It was observed that, for the studied porphyrins, the formation potential of the dianion radical is influenced by the electrodonor effect of the porphyrin substituents. Furthermore, the dianion radical of B is thermodynamically easier to obtain than that of A.

The metallization of A seems to have been reached, but the purification process needs to be improved. The electrolytic efficiency is approximately 94%. Spectroscopic techniques confirm that the metallization of B was reached. The reaction yield is 37% and the electrolytic efficiency is approximately 90%.

References

1. J. Longo, S. Lozzi, A. Simioni, P. Morais, A. Tedesco and R. Azevedo, *J. Photochem. Photobiol.* B., 94 (2009) 143.

2. J. Stukavec, V. Duchac, L. Horak, L.; P. Pouckova, *Photomed. Laser Surg*., 27 (2009) 107.
3. S. Pushpan, S. Venkatraman, V. Anand, J. Sankar, D. Parmeswaran, S. Ganesan, T. Chandrashekar, *Curr. Med. Chem. Anticancer Agents*, 2 (2002) 187.
4. K. Hosomizu, M. Oodoi, T. Umeyama, Y. Matano, K. Yohsida, S. Isoda, M. Isosomppi, N. Tkachencko, H. Lemmetyinen, I. Imahori, *J. Phys. Chem. B*, 112 (2008) 16517.
5. R. Chandra, M. Tiwari, P. Kaur, K. Sharma, R. Jain, S. Dass, *Indian J. Clin. Biochem.*, 15 (2000) 183.
6. B. Bandgar, P. Gujarathi, *J. Chem. Sci*., 120 (2008) 259.
7. M. Ribeiro, G. Azzellini, *J. Braz. Chem. Soc*., 14 (2003) 914.
8. W. White, R. Plane, *Bioinorg. Chem*., 4 (1974) 21.
9. L. Madriz, H. Carrero, J. Herrera, A. Cabrera.; N. Canudas, L. Fernández, *Top Catal.*, 54 (2011) 236.
10. K. Kadish, Q. Xu, J. Anderson, *ACS Symp. Ser*., 378 (1988) 451.
11. A. Vecchio-Sadus, *J. Appl. Electrochem*., 23 (1993) 404.
12. C. Saboureau, M. Troupel, J. Perichon, *J. Appl. Electrochem*., 20 (1990) 97.
13. A. Giraudeau, L. Ruhlmann, L. El Kahef, M. Gross, *J. Am. Chem. Soc*., 118 (1996) 2969.
14. T. Magdesieva, O. Nikitin, R. Abdullin, O. Polyakova, A. Yakimanskiy, M. Goikhman, I. Podeshvo, *Russ. Chem. Bull*., 58 (2009) 1423.
15. C. Yang, S. Lin, H. Chen, C. Chang, *Inorg. Chem*., 19 (1980) 3541.
16. L. Blanco, L. González, B. Kharisov, E. Aguilera, A. Garnovskii, F. Longoria, J. Costamagna, G. Borodkin, M. Korobov, *Synth. React. Inorg. Met.-Org. C*hem, 38 (2008) 503.
17. L. Blanco, E Aguilera, A. Huerta, L. Obregón, *Port. Electrochim. Act*, 27 (2009) 317.
18. I. Koç, M. Çamur, M. Bulut, R. Özkaya, *Can. J. Chem.*, 88 (2010) 375.
19. P. Krawczyk, J. Skowroński, *J. App. Electrochem.*, 40 (2010) 91.
20. L. Hernández, P. Hernández, V. Velasco, *Anal. Bioanal. Chem.*, 377 (2003) 262.
21. J. Fuhrhop, K. Kadish, D. Davis, *J. Amer. Chem. Soc.*, 95 (1973) 5140.
22. J. Manassen, A. Wolberg, *J. Amer. Chem, Soc*., 92 (1970) 2982.
23. M. Schiavon, L. Iwamoto, A. Ferreira, Y. Imamoto, M. Zanoni, M. Assis, *J. Braz. Chem. Soc.*, 11 (2000) 458.
24. D. Anjo, K Corkery, E. González, K. Marantos, K. Estrada, *J. Chem. Eng. Data*, 39 (1994) 813.
25. S. Shkirman, K. Solov'ev, T. Kachura, S. Arabei, E. Skakovskii, *J. Appl. Spectros*., 66 (1999) 68.
26. G. Wilkinson, Comprehensive Coordination Chemistry, *Pergamon Press, Oxford* (1987).

© 2012 by ESG (www.electrochemsci.org)